Proceedings of the 21st ICSMGE, Vienna, Austria, 14 – 19 June 2026. Pistrol, Adam & Schweiger (eds.)
Published by: ÖGG, Austrian Society for Geomechanics, Salzburg, Austria, ISBN 978-3-9503898-4-5
https://doi.org/10.53243/ICSMGE2026-1539

A Novel In-Situ CPT-based Test to Assess Deformability of Soils

Sebastien Volcy, Christophe Dano, Luc Sibille, Bruno Chareyre
Univ. Grenoble Alpes, CNRS, Grenoble INP, 3SR F-38000, Grenoble, France, sebastien.volcy@3sr-grenoble.fr

Hamid Hosseini-Sadrabadi
Equaterre: Geotechnical Design Office, Annecy, France

ABSTRACT: This paper introduces a novel in-situ test based on the Cone Penetration Test (CPT), aiming to characterize soil deformability directly, without relying on correlations. The test involves a penetrometer with a cone which is movable independently of the bars (above the cone). It mainly consists of applying force-controlled cycles of increasing amplitudes to the soil through the cone, the bars being at rest. Key findings reveal a pseudo-elastic domain where the cone exhibits minimal irreversible displacements under low cyclic forces. The force-displacement curve slopes in this region remain consistent, indicating a limited degradation of the soil deformation modulus. Beyond a threshold cycle force, significant plastic displacements occur, accompanied by a marked decrease of the deformation modulus.

KEYWORDS: In-situ Test, CPT, Deformation Modulus, pseudo-Elastic Domain.

1 INTRODUCTION

The Cone Penetration Test (CPT) is particularly well-suited to measure soil strength parameters, which is typically done in practice using measurements of the tip resistance q_c, the sleeve friction f_s, and the pore water pressure u in the case of a CPTu. As such, it is a perfectly viable test for geotechnical design calculations at the Ultimate Limit State (ULS).

Nonetheless, works have been undertaken on deriving soil deformation modulus from CPT data, either through empirical or semi-empirical correlations, or through dedicated CPT-based tests. The latter includes the Cone Loading Test (CLT) proposed by Faugeras et al. (1983) and further developed successively by Zhou (1997), Arbaoui et al. (2006) and (Reiffsteck et al., 2009).

This paper presents the physical modeling of a non-standard CPT-based test, the Cyclic Reloading Penetration Test (CRPT), using a movable mechanical tip developed by EQUATERRE company (Riegel, 2017). The test begins with a monotonic penetration phase, similar to the CLT. Upon reaching a target depth, the tip is unloaded to a small fraction of q_c sufficient to maintain soil compression under it. Then, force-controlled cycles of increasing amplitude are applied to the tip alone.

This methodology allows the investigation of soil response under different stress levels below the tip. In addition, the proposed technology avoids the influence on results of friction between the penetrometer body and the surrounding soil.

2 THE PHYSICAL MODEL

2.1 *Experimental setup*

The experimental setup includes:

1. A penetrometer with a 60° conical tip (Figure 1) and 4 cm² cross-sectional area (radius $r_p \approx 11.3$ mm) is used. The mechanical tip is linked to internal rods sliding within outer tubes, allowing it to move independently from the penetrometer body.
2. A calibration chamber measuring 1.28 m in height and 58.8 cm in internal diameter (Figure 2).
3. A loading system (Figure 2) comprising two actuators: a global one for standard monotonic penetration via the external tubes, and a local one for cyclic loading of the tip by moving the internal rods independently. This setup isolates the tip loading from the rest of the penetrometer body and eliminates tube-soil friction effects on the measurements.
4. Force and displacement sensors located at the level of the actuators, connected to a data acquisition system, that measure the applied force and tip position.

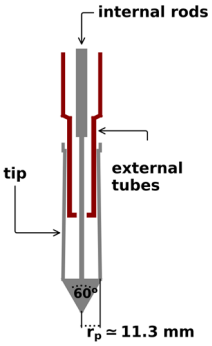

Figure 1. Schematic view of the mechanical tip used.

2.2 *Tested soil and sample preparation*

Tests were conducted on GA39 Fontainebleau sand (provided by Sibelco company), a fine sub-rounded to rounded sand with a median grain size diameter d_{50} of 113µm, about 200 times smaller than the tip diameter, and a uniformity coefficient C_u of 1.2 (Hosseini-Sadrabadi, 2019).

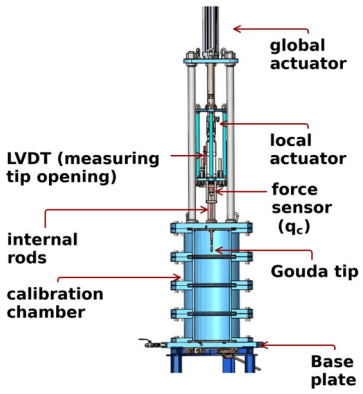

Figure 2. Exploded view of the experimental setup.

Soil samples are prepared by depositing sand to fill the calibration chamber. A low drop height of a few centimeters produces a loose sample. To achieve a dense sample, each approximately 5 cm-thick layer of sand is compacted manually using 30 blows from a square masonry tamper. Such a preparation method was adopted after many attempts with our pluviator fail as, due to the fine size of the particles, vortex was systematically induced in the granular flow.

For a given sample, its initial relative density $D_{r,0}$, estimated before any loading and assumed to be uniform throughout the calibration chamber, is determined from the total mass of sand used to fill the latter.

2.3 *Boundary conditions*

The boundaries of the chamber are considered perfectly rigid, preventing normal displacements along both the cylindrical wall and the chamber base surface. In contrast, the top surface of the sample is free of stress.

3 TEST METHODOLOGY AND TYPICAL SOIL RESPONSES

The test is carried out in three steps:

- First, the penetrometer is driven into the soil down to a target depth. The tip resistance q_c is recorded at this stage. Then, the global actuator, initially engaged for penetration, is immobilized.
- Second, the tip is unloaded via the local actuator to a small fraction of q_c, sufficient to keep the soil beneath the tip in compression. This fraction is here arbitrarily set to 5%.
- Finally, the soil is cyclically reloaded, still using the local actuator. Since the internal rods are directly connected to the tip, only the latter is mobilized. Force-controlled reloading cycles with increasing amplitudes are applied. For any two cycles, the ratio of their periods is equal to the ratio of their amplitudes, thus ensuring a constant stress loading and unloading rate of the tip.

The cycles are performed sufficiently slowly – with 60s as the execution time of the first cycle– to ensure a quasi-static regime and fully drained conditions (the latter, in case of fully saturated soils). The measured tip velocity is actually of the order of 10^{-4} m/s to 10^{-3} m/s throughout the test.

The reloading cycles are triangular, as shown in Figure 3 for one test, presenting the normalized tip stress q/q_c, or equivalently the normalized force F/F_c on the tip with time t, F_c being the force associated to q_c.

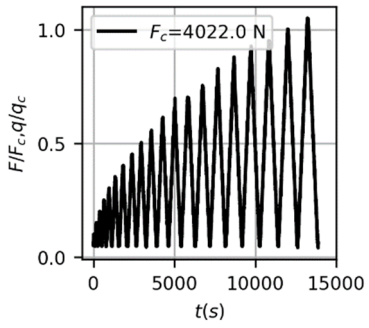

Figure 3. Reloading cycles: time series of the tip stress.

Figure 4 and Figure 5 respectively show the typical normalized tip displacement w/r_p versus the time t and the normalized tip stress q/q_c versus the normalized displacement w/r_p.

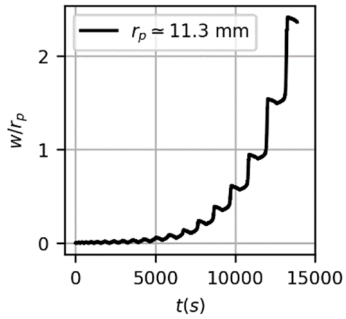

Figure 4. Tip displacement during the reloading cycles.

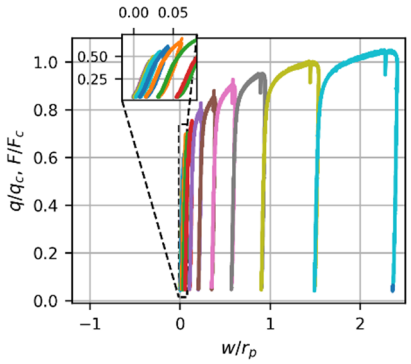

Figure 5. Deformability curve representing soil response to the cycles.

Figure 6 presents a typical cycle extracted from the soil response during cyclic loading as shown in Figure 5 (which includes about twenty cycles). Parts AB and BC of the cycle correspond respectively to the loading and the unloading phases. The irreversible displacement of the tip over a cycle is represented by segment AC and is denoted δ_i in the following. The reloading modulus discussed later, is related to the slope S_c of line AB, referred to as the soil secant stiffness.

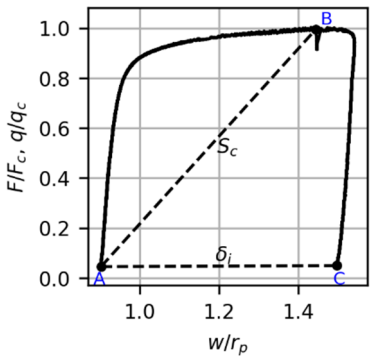

Figure 6. Definition of two relevant variables on one arbitrary cycle.

4 RESULTS AND DISCUSSIONS

The results presented here correspond to two tests which are described in Table 1. The nomenclature of the compacity

follows the standard NF P 94-059 and the relative density is computed with $e_{min} = 0.56$ and $e_{max} = 1.03$ (Silva, 2014).

Table 1. Brief description of the carried CRPTs.

Label	$D_{r,0}$[-]	Compacity	q_c(MPa)
CRPT 1	0.02	Very loose	0.27
CRPT 2	0.70	Dense	6.75

4.1 *Pseudo-Elastic Domain*

Figure 7 presents the normalized tip irreversible displacement δ_i/r_p versus the stress amplitude normalized by q_c over the cycles, for the two tests. As observed, two distinct stress domains can be differentiated. Within the first one, determined by low normalized amplitude cycles, the tip nearly returns to its initial position at the end of a cycle. Beyond a certain threshold, however, the incremental irreversible displacements of the tip begin to increase progressively with each cycle. This marks the onset of the second domain, where increasingly larger deformations occur in the soil, eventually leading to failure. The first domain, characterized by such an absence of significant plastic deformations at the macroscopic scale as described, defines a pseudo-Elastic domain, which is relevant to SLS design.

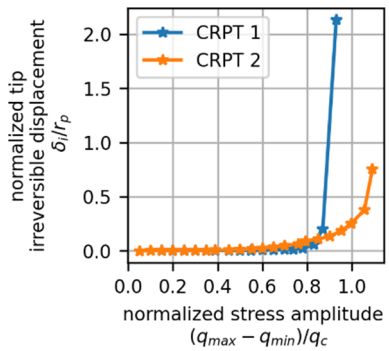

Figure 7. Tip irreversible displacements over the cycles.

Figure 8 presents S_c, normalized by its initial value S_0, versus the normalized stress amplitude, over the cycles. The results show the test ability to assess the degradation of the soil deformation modulus with the stress level (or equivalently the strain level).

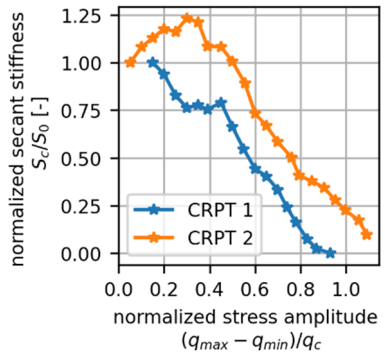

Figure 8. Secant stiffness degradation over the cycles.

4.2 *Penetrometer modulus*

A deformation modulus, denoted E_{pn} and termed as the penetrometer modulus to follow Reiffsteck (2009), may be derived from S_c per the relation:

$$E_{pn} = \frac{S_c}{r_p}\frac{(3-4\nu)(1+\upsilon)}{4\pi(1-\upsilon)} \qquad (1)$$

As done in Faugeras et al. (1983) among others, this relation originates in an interpretation of the test following the Kelvin's theoretical problem of a concentrated load applied in an interior point to a semi-infinite elastic medium (Mindlin, 1936). The tip is assimilated to a rigid circular plate, indefinitely embedded in a soil volume which is assumed to be isotropic, homogeneous, linear elastic of characteristics E and υ.

Within the SLS stress domain, E_{pn} can be reasonably considered as a pseudo-elastic modulus; it is denoted as such to avoid any confusion with the Young modulus E, which is a purely elastic modulus. However, beyond the stress threshold initiating significant tip irreversible displacements, E_{pn} is a plastic secant modulus, integrating soil plastic deformations.

Figure 9 shows E_{pn}, computed with υ taken as 0.33, versus the normalized stress amplitudes all over the cycles. It can be well observed the ability of the test to assess the effect of the soil density on its deformability.

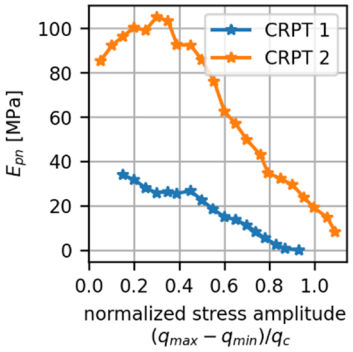

Figure 9. Degradation curves of the penetrometer modulus.

4.2.1 *Testing methodology validation.*

Two triaxial tests with unloading/reloading cycles were conducted to validate the testing and interpretation methodology developed through the progressive CRPT program. The test matrix is summarized in Table 2. The tests samples are dry, they have similar initial relative densities $D_{r,0}$ but two different consolidation stresses p_0.

Table 2. Summary of the triaxial tests with unloading/reloading cycles of increasing amplitudes.

Label	$D_{r,0}$[-]	p_0(kPa)	q_{peak}(kPa)
TX 1	0.57	50	189.5
TX 2	0.50	100	290.9

Each test begins with isotropic consolidation, followed by monotonic shearing until the deviatoric stress q reaches a fraction of the peak shear strength q_{peak}. The sample is then unloaded until q reaches a minimum value q_{min}. Subsequently, a series of reloading/unloading cycles is applied, at a rate of 0.2 mm/min. Their amplitudes increase progressively by 25 kPa, and the lower bound q_{min} of q is kept constant.

Figure 10 compares the evolutions of the secant modulus E_s, obtained from the cyclic triaxial tests and of E_{pn}. E_s is computed from the peak-to-peak stress and strain values of each cycle, exactly as it is done for the CRPTs. Both are plotted over the cycles, against the stress amplitude normalized by q_{peak} for the triaxial tests and by q_c for the CRPTs. The choice of plotting the moduli versus the stress rather than the strain levels comes

from the inconsistency of the notion of strain around the penetrometer tip.

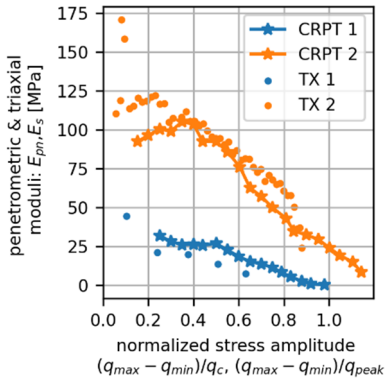

Figure 10. Comparison between penetrometer modulus and triaxial secant modulus on all the cycles.

The results reveal a remarkable overlap between the degradation trends observed in both testing approaches. This agreement not only confirms the consistency of the CPT-derived stiffness measurements but also validates the use CRPT as a reliable method for evaluating cyclic soil behavior regarding its deformability. Notably, as observed in Figure 11, the initial stiffness values in the triaxial tests correspond to strain levels of the order of 10^{-3} where the soil remains essentially elastic, further supporting the ability of the cyclic reloading CPT to address soil deformability in a pseudo-elastic domain.

Notably, this subdomain, comprising typically the first 4 cycles, spans over around 10 minutes, highlighting the efficiency of the developed test and methodology.

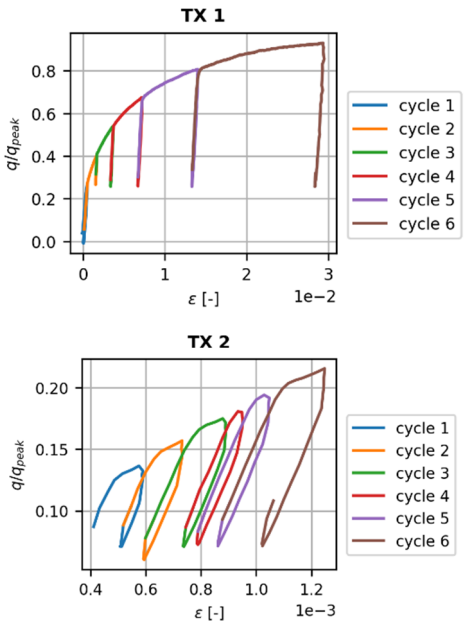

Figure 11. Shearing curves corresponding to the triaxial tests.

5 CONCLUSIONS

In this paper was presented the CRPT (Cyclic Reloading Penetration Test), a novel in-situ CPT-based test to assess soil deformability. The methodology involves a tip that is movable independently from the remaining part of the penetrometer, eliminating thereby the effect of the friction between the latter and the surrounding soil. The test consists mainly of applying force-controlled cycles on the tip, with increasing amplitudes.

The main results reveal the test ability (1) to assess the soil stiffness degradation with strains prior to failure, (2) to identify a stress domain associated to a pseudo-elastic behavior of the soil, thus of relevance for Service Limit State design and (3) to allow for the determination of a pseudo-elastic modulus, necessary for settlement estimations, without correlations. Moreover, if only the pseudo-elastic deformation modulus is of interest, and not the entire degradation curve, the test can be completed in ten minutes, once the target depth is reached.

However, the following remarks should be kept in mind, as they define the limitations of the presented results and highlight several potential areas for improving the test, as it will be addressed in future works:

1. The deformation of the internal rods and of the contacts between them, may affect the tip position measurements, as these are not taken at the tip level itself. This effect becomes more significant in dense soils. A subsequent correction, relatively to the loading system compliance shall be applied to the measured tip displacement to assess soil deformability with better accuracy.
2. Also, since the force is not measured directly at the tip, its measurement inherently includes the effects of inter-rod friction and/or misalignment. Furthermore, although the influence of friction between the soil and the stationary external tubes has been eliminated, the recorded values still account for friction between the soil and the sleeve behind the cone. These issues could be addressed by using an electric cone for instance.
3. The results presented here come from CRPTs carried out in dry samples of a given sand, under laboratory controlled conditions, with no effect of the vertical in-situ stress. Further validation requires in-situ testing under natural soil conditions.

6 REFERENCES

Arbaoui, H., Gourvès, R., Bressolette, P., Bodé, L. 2006. Mesure de la déformabilité des sols in situ à l'aide d'un essai de chargement statique d'une pointe pénétrométrique. *Canadian geotechnical journal* 43, 355–369.

Hosseini-Sadrabadi, H. 2019. Identification in-situ des sols liquéfiables par pénétromètre statique cyclique: modélisations physiques et numériques. PhD thesis, Université Grenoble Alpes.

J.-C Faugeras, G Fortuna, and R Gourvès. 1983. Mesure de la compressibilité des sols à l'aide du pénétromètre statique. In *Reconnaissance des Sols et des Roches par Essais en place. Symposium International, Paris*, France, 269–274.

Matias Felipe Silva Illanes. 2014. Experimental study of ageing and axial cyclic loading effect on shaft friction along driven piles in sands. PhD thesis. Université Grenoble Alpes.

Raymond D Mindlin. 1936. Force at a point in the interior of a semi-infinite solid. Physics, 7(5), 195–202.

Reiffsteck, P. H., Thorel, L., Bacconnet, C., Gourves, R., & Van De Graaf, H. C. 2009. Measurements of soil deformation by means of cone penetrometer. *Soils and foundations*, *49*(3), 397-408.

Riegel, P. 2017. Pénétromètre statique pour l'évaluation du caractère liquéfiable d'un sol et procédés associés. Dépôt de brevet FA841687 18.

Shuhua Zhou. 1997. Caractérisation des sols de surface à l'aide du pénétromètre dynamique léger à énergie variable type "Panda". PhD thesis, Clermont-Ferrand 2.

NF P 94-059. 2000. Sols Reconnaissance et essais détermination des masses volumiques minimale et maximale des sols non cohérents. *Editions AFNOR Boutique, Saint-Denis, France.*